Connectivity-aware sectional visualization of 3D DTI volumes using perceptual flat-torus coloring and edge rendering

Çağatay Demiralp[1] Song Zhang[1] David F. Tate[1] Stephen Correia[1] David H. Laidlaw[1]

[1]Brown University, Providence, RI, USA

Abstract

*We present two new methods for visualizing cross-sections of 3D diffusion tensor magnetic resonance imaging (DTI) volumes. For each of the methods we show examples of visualizations of the corpus callosum in the mid-sagittal plane of several normal volunteers. In both methods, we start from points sampled on a regular grid on the cross-section and, from each point, generate integral curves in both directions following the principal eigenvector of the underlying diffusion tensor field. We compute an anatomically motivated pairwise distance measure between each pair of integral curves and assemble the measures to create a distance matrix. We next find a set of points in a plane that best preserves the calculated distances that are small—each point in this plane represents one of the original integral curves. Our first visualization method wraps this planar representation onto a flat-torus and then projects that torus into a visible portion of a perceptually uniform color space (L*a*b*). The colors for the paths are used to color the corresponding grid points on the original cross-section. The resulting image shows larger changes in color where neighboring integral curves differ more. Our second visualization method lays out the grid points on the cross section and connects the neighboring points with edges that are rendered according to the distances between curves generated from these points. Both methods provide a way to visually segment 2D cross sections of DTI data. Also, a particular contribution of the coloring technique used in our first visualization method is to give a continuous 2D color mapping that provides approximate perceptual uniformity and can be repeated an arbitrary number of times in both directions to increase sensitivity.*

1. Introduction

Diffusion-Tensor Magnetic Resonance Imaging (DTI) enables the exploration of fibrous tissues such as brain white matter and muscles non-invasively *in-vivo*. It exploits the fact that water in these tissues diffuses at faster rates along the fibers than orthogonal to them. However, the multivalued nature of DTI data poses challenges in visualizing and understanding the underlying structures. Integral curves that represents neural pathways by showing paths of fastest diffusion are among the most common information derived from DTI volumes. They are generated by tracking the principal eigenvector of the underlying diffusion tensor field in both directions. They are often visualized with streamlines or variations of streamlines (streamtubes and hyperstreamlines) in 3D. In this paper, we present two new methods for visualizing cross sections of DTI volumes that incorporate the 3D out-of-plane connectivity information typically conveyed by the integral curves (see Fig. 1). Slice-based 2D visualizations of scientific data are generally effective, fast and synoptic [CM02, SWD04]. Also, looking at 2D cross-sections is still the most common practice by far among scientists and physicians for data exploration. Furthermore, there is some anecdotal evidence that incorporation of 2D cross-sections in 3D visualizations of medical data sets data is preferred by the same group [DJK*06].

For each of our visualization methods we show examples of visualizations of the corpus callosum in the mid-sagittal plane of three normal volunteers. The corpus callosum is the largest white matter fiber bundle in the brain and a target for clinical and neuroscience research into normal developmental vs. pathological changes in white matter integrity across the lifespan and the functional correlates of those changes. Distinct cross-sectional regions of the corpus callosum may contain fibers that subserve specific cognitive or behavioral functions mediated by the cortical regions to which they project. Proxy measures (e.g., thickness, volume, area, shape) of the health of these cross-sectional regions may correlate with measures of the cognitive and behavioral functions they subserve. In fact, the corpus callosum has been shown to differ on such measures by handedness, gender, and age as well as in disorders such as Alzheimer's disease and schizophrenia [HJL*04].

2. Related Work

Mapping colors to data values is a fundamental operation in scientific visualization. Previous work based on empirical studies addressed the problem of generating perceptu-

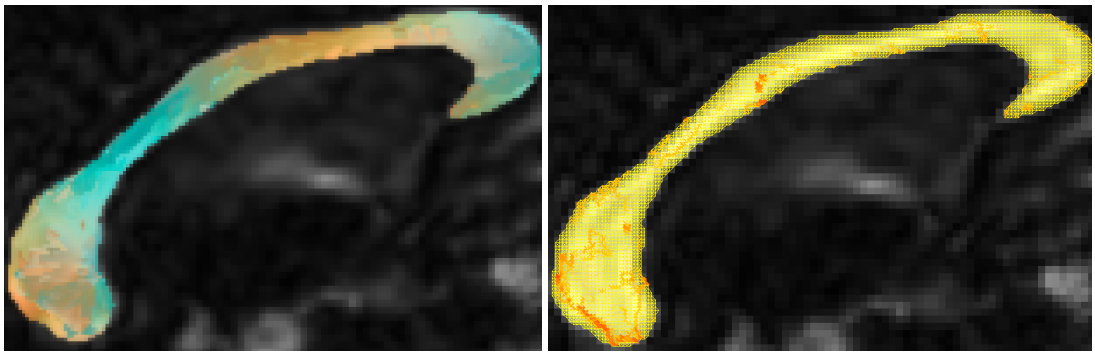

Figure 1: *Flat-torus coloring (left) and edge rendering (right) visualizations of the mid-saggital plane of the corpus callosum in a normal person's brain*

ally effective colormaps [War88, Hea96, LH92, KRC02]. We use the CIE L*a*b* color space that is a perceptually uniform (approximately) color space proposed by the Commission Internationale de l'Eclairage (CIE) in 1976. A color space is said to be perceptually uniform if the perceptual difference between any two colors in just noticeable difference (JND) units is equal to the Euclidean distance in that color space. Several different geometric models, including line, plane, cone, cylinder, and B-spline surfaces have been proposed for univariate, bivariate or trivariate color mapping [Pha90, Rob88]. We extend the earlier models by introducing the flat-torus model to give a continuous 2D color mapping that is approximately uniform and that can be repeated an arbitrary number of times in both directions to increase sensitivity. Integral curves generated from DTI volumes have been visualized generally with streamlines in 3D with different geometric (i.e., hyperstreamlines, streamtubes, etc.) and coloring combinations. In a work that is conceptually partly similar to our work, Brun *et al.* colored DTI integral curves by embedding them in 3D RGB space using a non-linear dimensionality reduction technique [BPKW03]. Volume visualization of DTI data included isosurface extraction and volume rendering. Previous cross-sectional visualizations of DTI mapped glyphs (box, ellipsoid and superquadratic) and colors to tensor voxels [ZKL04]. Pajevic *et al.* proposed methods to colormap DTI cross-sections according to principle eigenvectors of tensor voxels using different color spaces, including perceptually uniform CIE L*u*v color space. The authors point at the potential limitations due to the irregularity of the L*u*v space. Our flat-torus model addresses some of the limitations discussed in this work [PP99].

3. Methods

In both visualization methods presented here, we start from points (seeds) sampled on a regular grid on the cross-section and, from each point, generate integral curves in both directions following the principal eigenvector of the underlying diffusion tensor field. We compute an anatomically motivated pairwise distance measure between each pair of integral curves and assemble the measures to create a distance

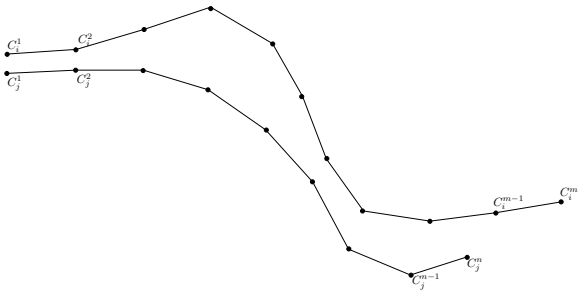

Figure 2: *Polyline representations of two integral curves C_i and C_j*

matrix. The distance matrix is utilized by the both methods to convey the out-of-plane connectivity information. We explain how we measure distances between the integral curves to construct the distance matrix in the next section.

3.1. Distance Measure Between Integral Curves

Integral curves generated from DTI volumes are solutions to the first-order differential equation $\frac{dC}{ds} = \vec{v}_1(C(s))$, where s parameterizes the curve and v_1 is the principal eigenvector at the point $C(s) = (x(s), y(s), z(s))$. We compute the integral curve $C(s)$ passing through a given seed point $C(0)$ (initial conditions) by integrating the above equation for $s > 0$ and $s < 0$ (i.e., both directions from the seed point). There have been different distance measures proposed for integral curves generated from DTI volumes [MVvW05]. In the current work we adapt a measure proposed by Zhang *et al.* with a slight modification [ZDL03]. The measure is anatomically motivated in that it is designed to increase whenever one path has points that are not near the other path. Note that our measure does not necessarily satisfy triangle inequality, therefore, it is not a metric. Given any two integral curves C_i and C_j that are represented as polylines with m and n vertices respectively (like the ones shown in Fig. 2), we first find mean distances d_{ij} and d_{ji} then, determine the maximum of these two distances as the distance D_{ij} between the two curves:

$$d_{ij} = \frac{\sum_{k=1}^{m} dist(C_i^k, C_j)}{m}, \quad d_{ji} = \frac{\sum_{k=1}^{n} dist(C_j^k, C_i)}{n} \tag{1}$$

$$D_{ij} = D_{ji} = max(d_{ij}, d_{ji}) \tag{2}$$

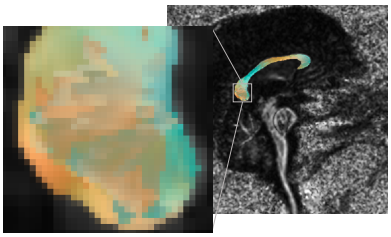

Figure 3: *Flat-torus coloring of the mid-sagittal of the corpus callosum in a normal person's brain*

Figure 4: *Seed points are adjusted so that Euclidean distances between the points on the plane reflect the distances between their associated integral curves.*

The function $dist(p,C)$ returns the shortest Euclidean distance between the point p and curve C. We compute distance between each pair of integral curves as we denoted and assemble the measures to create a distance matrix. The distance matrix is a real positive symmetric matrix with zeros along the diagonal.

3.2. Flat-Torus Coloring

The goal of our first method is to reflect the boundaries in distance differences in the data as perceptual boundaries. For this, we lay out the seed points on a plane and adjust their positions using a simple mass-spring-based optimization algorithm so that the calculated distances between their associated integral curves are best preserved locally. Fig. 4 illustrates how seed point coordinates change after running the optimization algorithm. We coordinate-transform the adjusted points using principle component analysis (PCA) to have a succinct representation. Finally, we wrap this planar representation onto a flat torus and then projects that torus into a visible portion of the CIE L*a*b* space. A flat-torus in 4-space is a Cartesian product of two circles in R^2. It can be obtained by a mapping $W : R^2 \rightarrow R^4$ such that

$$W(x,y) = (u,v,z,t) = (r_1 \cos x, r_1 \sin x, r_2 \cos y, r_2 \sin y) \quad (3)$$

where $r1$ and $r2$ are the radii of the circles. The flat-torus has 0 Gaussian curvature everywhere (i.e., is a developable surface), therefore a plane can be wrapped around it without distortion [dC76].

We project the flat-torus to the visible partition of L*a*b* color space, centered at $(L_o, a_o + r_1, b_o + r_1)$ as follows:

$$L* = L_o + t, \;\; a* = a_o + r_1 + u + z, \;\; b* = b_o + r_1 + v + z \quad (4)$$

Note that this projection is not isometric. It has two lines of self-intersection (where different (x,y) points map to the same colors) as well as distorting the angles between the coordinate directions. We discuss this further in Sec. 4. For the examples shown in this paper, we locate the projected toric in the L*a*b interval $I = (I_L, I_b, I_c)$, where $I_L = [60,80], I_a = [-50,30], I_b = [-20,60]$ and use $r_1 = 10$, $r_2 = 40$. The resulting images show larger changes in color where neighboring integral curves differ more. One of the advantages of using this flat-torus projection is that we can adjust the sensitivity of the color mapping by rescaling point plane and wrapping around the two circles continuously.

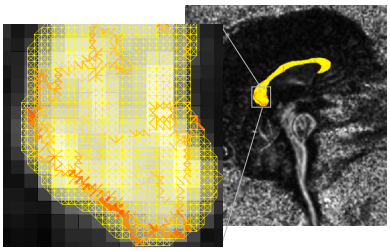

Figure 5: *Edge rendering visualization of the mid-sagittal plane of the corpus callosum in a normal person's brain.*

3.3. Edge Rendering

Our second visualization method lays out the grid points on the cross section and connects the neighboring points with edges that are rendered according to the distances between curves generated from these points. Note that we sample seed points on a rectilinear grid where the vertical and horizontal distances between the grid points are equal to δ. We define the seed points X_i and X_j to be neighbors if $||X_i - X_j||_2 = \delta$ or $||X_i - X_j||_2 = \delta\sqrt{2}$ (i.e., a seed point can have maximum 8 neighbors). Edges are drawn redder in color and thicker where neighboring seed points' integral curves differ more.

4. Results and Discussion

Figs. 3 and 5 show the visualizations of the same normal person's corpus callosum with close-up views of the same region. Notice the correspondance between regions in flat-torus coloring and edges in edge rendering. Other results from two DTI brain data sets are shown in Fig. 6. It is important to note that the perceptual uniformity in our color mapping is an approximation, because the flat-torus cannot be mapped to three dimensions isometrically. Our projection can deemphasize changes in certain regions of the flat torus. There are other projections that may be closer to isometric, and it also may be possible to add a fourth perceptual dimension like texture to the three color dimensions, removing the need for a projection and preserving the properties of the flat torus.

5. Conclusions

We have presented two new cross-sectional visualization methods. The primary strength of both methods is providing a compact and contextual visualization by bringing higher dimensional connectivity information onto a 2D plane which is effective and familiar to practitioners. We have applied

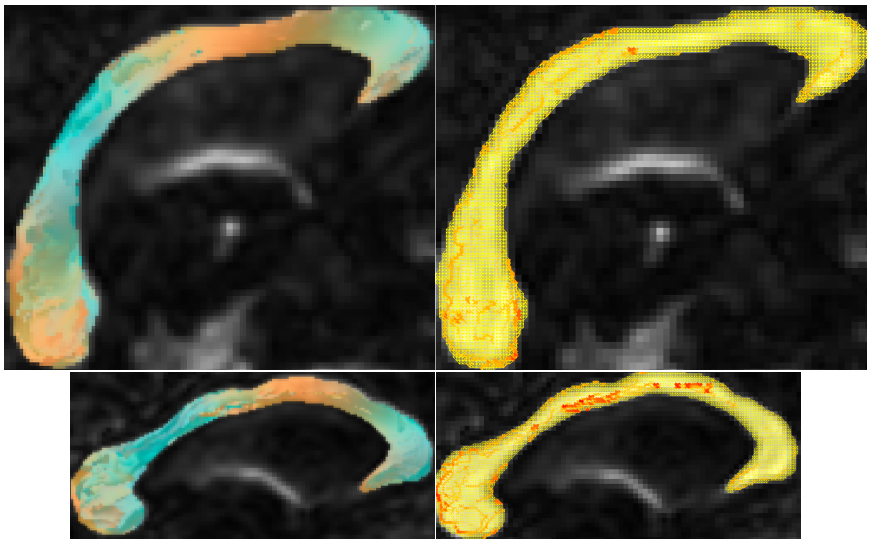

Figure 6: *Flat-torus coloring (left) and edge rendering (right) visualizations of the mid-saggital plane of the corpus callosum in two normal persons' brains.*

them to visually segment the mid-saggital cross-section of the corpus callosum in the brain. Feedback from neuroscientist collaborators suggests that our visualization methods can be useful in identification of smaller caliber anatomically or functionally related white-matter structures, particularly those that are contained within large bundles or fasciculi that project to multiple areas. Flat-torus coloring is a new geometric model for bivariate color mapping that is approximately uniform perceptually and that can be repeated an arbitrary number of times in both directions. The underlying idea of this work can be extended to visualization of other vector, tensor or multi-scalar data volumes.

References

[BPKW03] BRUN A., PARK H.-J., KNUTSSON H., WESTIN C.-F.: Coloring of dt-mri fiber traces using laplacian eigenmaps. In *EUROCAST'03* (2003), pp. 564–572.

[CM02] COCKBURN A., MCKENZIE B.: Evaluating the effectiveness of spatial memory in 2d and 3d physical and virtual environments. In *CHI'02* (2002), pp. 203–210.

[dC76] DO CARMO M. P.: *Differential Geometry of Curves and Surfaces*. Prentice-Hall, 1976.

[DJK*06] DEMIRALP C., JACKSON C., KARELITZ D., ZHANG S., LAIDLAW D. H.: Cave and fishtank virtual-reality displays: A qualitative and quantitative comparison. *IEEE TVCG 12*, 3 (2006), 323–330.

[Hea96] HEALEY C. G.: Choosing effective colours for data visualization. In *VIS '96* (1996), pp. 263–ff.

[HJL*04] HWANG S. J., JI E. K., LEE E. K., KIM Y. M., DA Y. S., CHEON Y. H., RHYU I. J.: Gender differences in the corpus callosum of neonates. *Neuroreport 15*, 6 (2004), 1029–32.

[KRC02] KINDLMANN G., REINHARD E., CREEM S.: Face-based luminance matching for perceptual colormap generation. In *Procs. of Vis'02* (2002), pp. 299–306.

[LH92] LEVKOWITZ H., HERMAN G. T.: Color scales for image data. *IEEE CG&A 12*, 1 (1992), 72–80.

[MVvW05] MOBERTS B., VILANOVA A., VAN WIJK J. J.: Evaluation of fiber clustering methods for diffusion tensor imaging. In *Procs. of Vis'05* (2005), pp. 65–72.

[Pha90] PHAM B.: Spline-based color sequences for univariate, bivariate and trivariate mapping. In *Procs. of Vis'90* (1990), pp. 202–208.

[PP99] PAJEVIC S., PIERPAOLI C.: Color schemes to represent the orientation of anisotropic tissues from diffusion tensor data: Application to white matter fiber tract mapping in the human brain. *MRM 42* (1999), 526–540.

[Rob88] ROBERTSON P. K.: Visualizing color gamuts: A user interface for the effective use of perceptual color spaces in data displays. *IEEE CG&A 8*, 5 (1988), 50–64.

[SWD04] SAVAGE D. M., WIEBE E. N., DEVINE H. A.: Performance of 2d versus 3d topographic representations for different task types. In *HFES Annual Meeting* (2004).

[War88] WARE C.: Color sequences for univariate maps: Theory, experiments and principles. *IEEE CG&A 8*, 5 (1988), 41–49.

[ZDL03] ZHANG S., DEMIRALP C., LAIDLAW D. H.: Visualizing diffusion tensor MR images using streamtubes and streamsurfaces. *IEEE TVCG 9*, 4 (2003), 454–462.

[ZKL04] ZHANG S., KINDLMANN G., LAIDLAW D. H.: Diffusion tensor MRI visualization. In *Visualization Handbook*. Academic Press, June 2004.